Asymptotic Analysis for Dual-Hop Communication Networks with PSK and Imperfect CSI

Nikos C. Sagias*, Ranjan K. Mallik†, and Nikolaos D. Tselikas*
*Department of Informatics & Telecommunications, University of Peloponnese, Karaiskaki street, 22100 Tripoli, Greece (nsagias@ieee.org, ntsel@uop.gr)
†Department of Electrical Engineering, Indian Institute of Technology–Delhi, Hauz Khas, New Delhi 110016, India (rkmallik@ee.iitd.ernet.in)

***Abstract*—We develop an analytical framework for the end-to-end (e2e) asymptotic performance of pilot-symbol assisted M-ary phase-shift keying (M-PSK) dual-hop relaying communication networks. The relays use the selective-decode-and-forward protocol and are equipped with multiple receive antennas. Channel estimation per antenna branch is done based on the least-squares estimation technique by means of pilot symbols. Also, maximal-ratio combining and coherent detection are performed at the receiving end. Simple approximate average symbol error probability (ASEP) expressions are obtained for high signal-to-noise ratio (SNR) when $M \geq 2$. Our analysis is generic enough to account for any frequency-flat, time-selective, and/or arbitrarily correlated fading channel model per hop. As a case study, we provide e2e M-PSK ASEP expressions considering arbitrarily correlated Nakagami fading channels. Moreover, the optimal power allocation is studied, while the cooperation-gain and diversity-order are extracted. Numerical results are finally presented to verify the accuracy of our asymptotic expressions.**

***Index Terms*—Average symbol error probability (ASEP), channel state information (CSI), cooperative communications, correlated fading, decode-and-forward (DF), least-squares estimation (LSE), M-ary phase-shift keying (M-PSK), maximal-ratio combining (MRC), relays.**

I. Introduction

Cooperative networks promise high quality of services for next-generation communication systems [1]. Their end-to-end (e2e) performance can be further improved by employing multiple antennas relays and using efficient diversity schemes. When coherent detection is assumed, in practice, channel estimates are required, which are imperfect due to additive noise inserted from the estimation technique used, resulting to performance degradation. Therefore, it is important to study the effect of such imperfection on the e2e performance.

In the technical literature there are many important works on point-to-point communications considering pilot-symbol assisted modulation techniques, e.g., [2]–[8]. Motivated by these early works, various papers on cooperative communications with imperfect channel state information (CSI) have been published, e.g., [9]–[14], studying important aspects of relaying systems. However, due to specific assumptions and/or considerations, their generality is limited, e.g., by assuming a specific channel model, a single-channel scenario, uncorrelated channels, or a specific modulation order.

The error rate performance of M-ary phase-shift keying (M-PSK) systems assuming imperfect CSI can be analyzed directly from the distribution of the inner product of two complex Gaussian random vectors [2, Appendix C]. Following this approach in this paper, a key point in our analysis is the generalization of a theorem originally presented in [8], [15] for the joint characteristic function (CF) of the real and imaginary parts of the inner product of two independent complex Gaussian random vectors. Based on this generalization, we develop an analytical framework for the asymptotic e2e M-PSK error-rate performance of dual-hop and multi-relay cooperative networks. The selective-decode-and-forward (sDF) protocol is adopted, while we consider that the relays are equipped with an arbitrary number of receive antennas. Prior to data transmission, each relay estimates the CSI using the least-squares estimation (LSE) technique by means of pilot symbols. Then, coherent detection based on the maximal-ratio combining (MRC) scheme is performed. The inner-product approach appears to be a powerful tool, since it has the advantage of generality. Specifically, our analysis can be exploited assuming any time- and space-correlated channel model per hop, not-necessarily identical channels, and arbitrary number of antennas per receiving end. The only requirement is that it should be available the CF of the sum of squared fading envelopes for the channel model under consideration. Fortunately, for the most popular channel models, e.g., Rayleigh, Rice, and Nakagami, such an expression is readily available [8, eqs. (51) and (63)]. Finally, a case study based on our mathematical framework is presented considering correlated Nakagami fading.

II. Statistics of the Inner Product of Two Complex Gaussian Random Vectors

Theorem 1 (Inner Product of Two Mutually Independent Complex Gaussian Vectors): Let[1] $\mathbf{x} = [x_1\, x_2 \cdots x_L]^T$ and $\mathbf{y} = [y_1\, y_2 \cdots y_L]^T$ be two mutually independent complex Gaussian random vectors distributed as $\mathbf{x} \sim \mathcal{CN}(\boldsymbol{\mu}_\mathbf{x}, \mathbf{K}_\mathbf{x})$ and $\mathbf{y} \sim \mathcal{CN}(\boldsymbol{\mu}_\mathbf{y}, \mathbf{K}_\mathbf{y})$, respectively, where $\boldsymbol{\mu}_\mathbf{x} = \mathcal{E}_\mathbf{x}\langle\mathbf{x}\rangle =$

[1]Notations: $\mathbf{I}_L$ is the $L \times L$ identity matrix, $\mathbf{1}_L$ and $\mathbf{0}_L$ denote $L \times 1$ vectors of ones and zeros, respectively, $\otimes$ denotes the Kronecker product of matrices, $(\cdot)^T$ and $(\cdot)^H$ denote the transpose and Hermitian operators, respectively, $\mathbf{x} \sim \mathcal{CN}(\boldsymbol{\mu}_\mathbf{x}, \mathbf{K}_\mathbf{x})$ reads as "$\mathbf{x}$ is distributed as a complex normal vector with mean and covariance matrix $\boldsymbol{\mu}_\mathbf{x} = \mathcal{E}_\mathbf{x}\langle\mathbf{x}\rangle$ and $\mathbf{K}_\mathbf{x} = \mathcal{E}_\mathbf{x}\langle(\mathbf{x} - \boldsymbol{\mu}_\mathbf{x})(\mathbf{x} - \boldsymbol{\mu}_\mathbf{x})^H\rangle$, respectively," with $\mathcal{E}_\mathbf{x}\langle\cdot\rangle$ standing for the expectation over $\mathbf{x}$ operator, $(\cdot)^*$ denotes the complex conjugate, $\mathrm{tr}(\cdot)$ stands for the trace of a matrix, $\mathrm{Diag}\{\cdot\}$ stands for a square diagonal matrix, $\Re\{\cdot\}$ and $\Im\{\cdot\}$ denote the real and imaginary operators, respectively, $\jmath = \sqrt{-1}$, $\|\cdot\|$ denotes the Euclidean norm, and $\mathbb{R}$ and $\mathbb{C}$ are the set of real and complex numbers, respectively.

978-1-4799-3083-8/14/$31.00

$$\Psi_{z_\rho,z_\iota}\left(\jmath\,\omega_1,\jmath\,\omega_2\right)=\frac{\exp\left\{-\frac{\frac{\omega_1^2+\omega_2^2}{4}\,|q_i|^2\left(\left|\mu_{x_i}\right|^2\sigma_{y_i}^2+\left|\mu_{y_i}\right|^2\sigma_{x_i}^2\right)-\jmath\,\Re\left\{(\omega_1-\jmath\,\omega_2)\,\mu_{y_i}^*\,q_i\,\mu_{x_i}\right\}}{1+\frac{\omega_1^2+\omega_2^2}{4}\,|q_i|^2\,\sigma_{x_i}^2\,\sigma_{y_i}^2}\right\}}{\prod_{i=1}^{L}\left(1+\frac{\omega_1^2+\omega_2^2}{4}\,|q_i|^2\sigma_{x_i}^2\,\sigma_{y_i}^2\right)} \tag{2}$$

$[\mu_{x_1}\,\mu_{x_2}\cdots\mu_{x_L}]^T$, $\mathbf{K_x}=\mathrm{Diag}\{\sigma_{x_1}^2,\sigma_{x_2}^2,\ldots,\sigma_{x_L}^2\}$ and $\boldsymbol{\mu}_\mathbf{y}=\mathcal{E}_\mathbf{y}\langle\mathbf{y}\rangle=[\mu_{y_1}\,\mu_{y_2}\cdots\mu_{y_L}]^T$, $\mathbf{K_y}=\mathrm{Diag}\{\sigma_{y_1}^2,\sigma_{y_2}^2,\ldots,\sigma_{y_L}^2\}$, with $\sigma_{x_i}^2=\mathcal{E}_{x_i}\left\langle|x_i|^2\right\rangle-\mathcal{E}_{x_i}^2\left\langle|x_i|\right\rangle$, $\sigma_{y_i}^2=\mathcal{E}_{y_i}\left\langle|y_i|^2\right\rangle-\mathcal{E}_{y_i}^2\left\langle|y_i|\right\rangle\;\forall i=1,\ldots,L$. Also, let the complex random variable (rv) $z\in\mathbb{C}$ be given by the inner product of $\mathbf{y}$ and $\mathbf{Q}\,\mathbf{x}$, i.e.,

$$z=\mathbf{y}^H\,\mathbf{Q}\,\mathbf{x}=z_\rho+\jmath\,z_\iota\,, \tag{1}$$

with $z_\rho=\Re\{z\}$, $z_\iota=\Im\{z\}$, and $\mathbf{Q}=\mathrm{Diag}\{q_1,\,q_2,\ldots,q_L\}$ being a square diagonal matrix, $\mathbf{Q}\in\mathbb{C}^{L\times L}$. Then, the joint CF of z_ρ and z_ι is given by (2) (at top of this page).

The proof of the above theorem can be found in the Appendix A of [16]. Note that [8, eq. (2)] is a special case of (2) for $\mathbf{Q}=\mathbf{I}_L$, $\mathbf{K_x}=\sigma_x^2\,\mathbf{I}_L$, and $\mathbf{K_y}=\sigma_y^2\,\mathbf{I}_L$.

III. Cooperative System Model

We consider a dual-hop network where a source node $\mathcal{S}$ transmits M-PSK symbols to a destination node $\mathcal{D}$ both directly and through R relay nodes $\mathcal{R}_1$, $\mathcal{R}_2$,..., $\mathcal{R}_R$. The source is equipped with one antenna, the destination with L_0, and the pth relay with L_p ($p=1,2,\ldots,R$). The relays use the sDF protocol to forward the data received from the source to the destination. According to this protocol, a relay forwards the information signal only if it is able to correctly decode it (referred as *the relay is on*); otherwise it remains idle (referred as *the relay is off*). The overall $\mathcal{S}\rightarrow\mathcal{D}$ transmission of an M-PSK symbol is completed in $R+1$ time slots.

A. Dual-Hop Network

Let $s\in S$ be the information-bearing symbol that belongs to an M-PSK constellation $S=\{S_0,S_1,\ldots,S_{M-1}\}$, with M denoting the modulation order and $S_l=\exp\{\jmath\,2\,\pi\,l/M\}$, $l=0,1,\ldots,M-1$. Also let $2\,E_s$ denote the total energy per symbol transmitted as a sum by all nodes during $R+1$ time slots. The transmitted symbol energy in the $(\ell+1)$th time slot ($\ell=0,1,\ldots,R$) will be $\lambda_\ell\,2\,E_s$, with $\lambda_\ell\in(0,1)$ being the source ($\ell=0$) or the ℓth ($\ell\neq0$) relay to total transmit power ratio and $\sum_{\ell=0}^{R}\lambda_\ell=1$. The $L_p\times1$ sampled baseband complex signal vector received at relay $\mathcal{R}_p$ from $\mathcal{S}$ in the first time slot is given by

$$\mathbf{w}_p=s\,\sqrt{\lambda_0\,2\,E_s}\,\mathbf{g}_p+\boldsymbol{\nu}_p\,. \tag{3a}$$

In (3a) $\boldsymbol{\nu}_p\in\mathbb{C}^{L_p}$ is the additive white Gaussian noise (AWGN) vector, distributed as $\boldsymbol{\nu}_p\sim\mathcal{CN}\left(\mathbf{0}_{L_p},2\,N_0\,\mathbf{I}_{L_p}\right)$. Also, $\mathbf{g}_p=[g_{p,1}\,g_{p,2}\cdots g_{p,L_p}]^T$ stands for a random channel complex gain vector and is independent of $\boldsymbol{\nu}_p$. The elements of the Hermitian covariance matrix of $\mathbf{g}_p$ are $\mathbf{K}_{g_p}[i,j]=\mathcal{E}_{g_{p,i},g_{p,j}}\langle g_{p,i}\,g_{p,j}^*\rangle-\mathcal{E}_{g_{p,i}}\langle g_{p,i}\rangle\,\mathcal{E}_{g_{p,j}}^*\langle g_{p,j}\rangle=\varrho_{p,i,j}\,\sqrt{\Theta_{p,i}\,\Theta_{p,j}}$ for $i\neq j$, with $\varrho_{p,i,j}$ standing for the correlation coefficient between ith and jth channels ($i,j=1,2,\ldots,L_p$) and $\mathcal{E}_{g_{p,i}}\left\langle|g_{p,i}|^2\right\rangle=\Theta_{p,i}$ for the power of the ith channel between the source and the pth relay. Moreover, the $L_0\times1$ sampled baseband complex signal vector received at node $\mathcal{D}$ from $\mathcal{S}$ in the first time slot ($\ell=0$) or from $\mathcal{R}_\ell$ in the $(\ell+1)$th time slot ($\ell\neq0$) can be expressed as

$$\mathbf{r}_\ell=s\,\sqrt{\lambda_\ell\,2\,E_s}\,\mathbf{h}_\ell+\mathbf{n}_\ell\,. \tag{3b}$$

In (3b) $\mathbf{n}_\ell\in\mathbb{C}^{L_0}$ is the AWGN vector, distributed as $\mathbf{n}_\ell\sim\mathcal{CN}\left(\mathbf{0}_{L_0},2\,N_0\,\mathbf{I}_{L_0}\right)$. Also, $\mathbf{h}_\ell=[h_{\ell,1}\,h_{\ell,2}\cdots h_{\ell,L_0}]^T$ stands for a random channel complex gain vector and is independent of $\mathbf{n}_\ell$. The elements of the Hermitian covariance matrix of $\mathbf{h}_\ell$ are $\mathbf{K}_{h_\ell}[i,j]=\mathcal{E}_{h_{\ell,i},h_{\ell,j}}\left\langle h_{\ell,i}\,h_{\ell,j}^*\right\rangle-\mathcal{E}_{h_{\ell,i}}\langle h_{\ell,i}\rangle\,\mathcal{E}_{h_{\ell,j}}^*\langle h_{\ell,j}\rangle=\rho_{\ell,i,j}\,\sqrt{\Omega_{\ell,i}\,\Omega_{\ell,j}}$ for $i\neq j$, with $\rho_{\ell,i,j}$ standing for the correlation coefficient between ith and jth channels ($i,j=1,2,\ldots,L_0$) and $\mathcal{E}_{h_{\ell,i}}\left\langle|h_{\ell,i}|^2\right\rangle=\Omega_{\ell,i}$ for the power of the ith channel between the ℓth node and $\mathcal{D}$.

After the first time slot, each relay performs MRC with the number of antennas that is equipped. Also, after $R+1$ time slots, node $\mathcal{D}$ performs MRC with $L_0\times$(1+number of relays that are on) signals. Due to the similarity of (3a) and (3b), next, we continue our analysis with respect to (3b). Then, it shall be straightforward to transform any derived result to a new formula for the source to relay links based on (3a). We now define three new vectors $\mathbf{r}=[\mathbf{r}_0\;\mathbf{r}_1\;\mathbf{r}_2\cdots\mathbf{r}_R]^T$, $\mathbf{h}=[\mathbf{h}_0\;\mathbf{h}_1\;\mathbf{h}_2\cdots\mathbf{h}_R]^T$, and $\mathbf{n}=[\mathbf{n}_0\;\mathbf{n}_1\;\mathbf{n}_2\cdots\mathbf{n}_R]^T$. The concatenated received signal vector at $\mathcal{D}$ after $R+1$ slots is

$$\mathbf{r}=s\,\sqrt{2\,E_s}\,\mathbf{V}\,\mathbf{h}+\mathbf{n}\,, \tag{4}$$

where vector $\mathbf{h}\in\mathbb{C}^{L_0\,(R+1)}$ has mean vector and covariance matrix $\boldsymbol{\mu}_\mathbf{h}=[\boldsymbol{\mu}_{h_0}\,\boldsymbol{\mu}_{h_1}\,\boldsymbol{\mu}_{h_2}\cdots\boldsymbol{\mu}_{h_R}]^T$ and $\mathbf{K_h}=\mathrm{Diag}\{\mathbf{K}_{h_0},\;\mathbf{K}_{h_1},\;\mathbf{K}_{h_2},\ldots,\mathbf{K}_{h_R}\}$, respectively. In (4), $\mathbf{n}$ is the noise vector $\mathbf{n}\sim\mathcal{CN}\left(\mathbf{0}_{L_0\,(R+1)},2\,N_0\,\mathbf{I}_{L_0\,(R+1)}\right)$ and $\mathbf{V}\in\mathbb{R}^{L_0\,(R+1)\times L_0\,(R+1)}$ is a diagonal square matrix defined as $\mathbf{V}=\mathrm{Diag}\{\sqrt{\lambda_0}\,\mathbf{I}_{L_0},\,\sqrt{\lambda_1}\,\mathbf{I}_{L_0},\,\sqrt{\lambda_2}\,\mathbf{I}_{L_0},\ldots,\sqrt{\lambda_R}\,\mathbf{I}_{L_0}\}$.

B. Least-Squares Channel Estimation

Let $\mathbf{s}_p=[s_{p_1}\,s_{p_2}\cdots s_{p_K}]^T$ be the transmitted pilot symbols vector, that is known to all relays and the destination node prior to data transmission (transmission of s in (4)). According to (4), in the $k\,(R+1)$th time slot ($k=1,2,\ldots,K$), the concatenated received signal vector at node $\mathcal{D}$, corresponding to the kth pilot symbol transmission, can be expressed as $\mathbf{r}_{p_k}=s_{p_k}\,\sqrt{2\,E_p}\,\mathbf{V}\,\mathbf{h}+\mathbf{n}_{p_k}$, where $\mathbf{n}_{p_k}\sim\mathcal{CN}\left(\mathbf{0}_{L_0\,(R+1)},2\,N_0\,\mathbf{I}_{L_0\,(R+1)}\right)$ is the kth pilot AWGN concatenated vector and $2\,E_p$ is the total pilot symbols energy transmitted during $R+1$ time slots. Let $\mathbf{r}_p=[\mathbf{r}_{p_1}\,\mathbf{r}_{p_2}\cdots\mathbf{r}_{p_K}]^T$ and $\mathbf{n}_p=[\mathbf{n}_{p_1}\,\mathbf{n}_{p_2}\cdots\mathbf{n}_{p_K}]^T$ represent the concatenated received signal and AWGN vectors over K pilot transmissions,

respectively. Then from $\mathbf{r}_{p_k}$, the concatenated received pilot symbols vector at node $\mathcal{D}$ after $R+1$ time slots, $\mathbf{r}_p \in \mathbb{C}^{L_0\,(R+1)\,K}$, can be written as

$$\mathbf{r}_p = \sqrt{2\,E_p}\,\left(\mathbf{s}_p \otimes \mathbf{I}_{L_0\,(R+1)}\right)\,\mathbf{V}\,\mathbf{h} + \mathbf{n}_p\,. \tag{5}$$

From (5), the estimated CSI vector $\hat{\mathbf{h}} \in \mathbb{C}^{L_0\,(R+1)}$ by node $\mathcal{D}$ can be obtained as

$$\hat{\mathbf{h}} = \frac{1}{\sqrt{2\,E_p}\,K}\,\mathbf{V}^{-1}\,\left(\mathbf{s}_p^H \otimes \mathbf{I}_{L_0\,(R+1)}\right)\mathbf{r}_p\,. \tag{6}$$

By substituting (5) in the above equation yields

$$\hat{\mathbf{h}} = \mathbf{h} + \mathbf{e}\,, \tag{7}$$

where $\mathbf{e} = \mathbf{V}^{-1}\,\left(\mathbf{s}_p^H \otimes \mathbf{I}_{L_0\,(R+1)}\right)\mathbf{n}_p/(\sqrt{2\,E_p}\,K)$ is the estimation error vector and is independent of $\mathbf{h}$. Vector $\mathbf{e}$ is distributed as $\mathcal{CN}\left(\mathbf{0}_{L_0\,(R+1)}, \gamma_{\rm p}^{-1}\,\mathbf{V}^{-2}\right)$, with $\gamma_{\rm p} = K\,E_p/N_0$ being the average pilot-to-noise ratio (PNR) per pilot sequence and per time slot and $2\,N_0$ being the single-side noise power spectral density. In (7), the mean vector and the covariance matrix of $\hat{\mathbf{h}}$ are $\boldsymbol{\mu}_{\hat{\mathbf{h}}} = \boldsymbol{\mu}_{\mathbf{h}}$ and $\mathbf{K}_{\hat{\mathbf{h}}} = \mathrm{Diag}\{\mathbf{K}_{h_0} + \frac{1}{\lambda_0\,\gamma_{\rm p}}\,\mathbf{I}_{L_0}, \mathbf{K}_{h_1} + \frac{1}{\lambda_1\,\gamma_{\rm p}}\,\mathbf{I}_{L_0}, \ldots, \mathbf{K}_{h_R} + \frac{1}{\lambda_R\,\gamma_{\rm p}}\,\mathbf{I}_{L_0}\}$, respectively.

IV. End-to-End M-PSK ASEP Analysis

The on or off state for each of the R relays can be represented by a binary variable $b_{p,n}$. When the pth relay correctly decodes the received signal, $b_{p,n} = 1$, otherwise, $b_{p,n} = 0$. Regarding the binary states of all R relays in the network, there are 2^R different combinations that can be represented by a bit vector $\mathbf{b}_n = [b_{1,n}\,b_{2,n}\cdots b_{R,n}]$, with $n = 0, 1, \ldots, 2^R - 1$. Under this notation, $\mathbf{b}_0 = \mathbf{0}_R$ when all relays are off, while $\mathbf{b}_{2^R-1} = \mathbf{1}_R$ when all relays are on.

Following the approach presented in [1], the e2e ASEP can be expressed as a sum of the average probabilities of symbol errors over all different network states, i.e.,

$$P_{se,e2e} = \sum_{n=0}^{2^R-1}\,\mathcal{E}_{\mathbf{h}}\left\langle P_{se,\mathcal{D}}|\mathbf{b}_n\right\rangle \prod_{p=1}^{R}\Pr\{\mathcal{R}_p:\ \mathrm{on/off}|b_{p,n}\}\,, \tag{8}$$

where $\mathcal{E}_{\mathbf{h}}\left\langle P_{se,\mathcal{D}}|\mathbf{b}_n\right\rangle$ denotes the ASEP at node $\mathcal{D}$ (averaged on $\mathbf{h}$), with cooperation of those relays that according to $\mathbf{b}_n$ are on. $\Pr\{\mathcal{R}_p:\ \mathrm{on/off}|b_{p,n}\}$ is the probability that the pth relay is on or off according to the $b_{p,n}$ value and is equal to

$$\Pr\{\mathcal{R}_p:\ \mathrm{on/off}|b_{p,n}\} = \left\{\begin{array}{c} \mathcal{E}_{\mathbf{g}_p}\left\langle P_{se,\mathcal{R}_p}\right\rangle, \quad \text{if } b_{p,n}=0 \\ 1-\mathcal{E}_{\mathbf{g}_p}\left\langle P_{se,\mathcal{R}_p}\right\rangle, \ \text{if } b_{p,n}=1\,, \end{array}\right. \tag{9}$$

with $\mathcal{E}_{\mathbf{g}_p}\left\langle P_{se,\mathcal{R}_p}\right\rangle$ being the ASEP (averaged on $\mathbf{g}_p$) for the $\mathcal{S}\to\mathcal{R}_p$ link. As earlier mentioned, next, we focus on the derivation of $\mathcal{E}_{\mathbf{h}}\left\langle P_{se,\mathcal{D}}|\mathbf{b}_n\right\rangle$ that is based on (3b). It shall become obvious that the same expressions can be also used to extract $\mathcal{E}_{\mathbf{g}_p}\left\langle P_{se,\mathcal{R}_p}\right\rangle$ for any $\mathcal{S}\to\mathcal{R}_p$ link.

A. Coherent Detection at the Destination Node

The reception of K pilot symbols per channel block transmitted by the $R+1$ nodes is followed by symbol-by-symbol reception and coherent detection of data in the destination node. For a transmitted data symbol s in a symbol interval, the signals received over $L_0\,(R+1)$ diversity branches, as given by vector $\mathbf{r}$ in (4), are combined using MRC. Assuming that the network is in state $\mathbf{b}_n$, the combiner output will be $\hat{\mathbf{h}}^H\,\boldsymbol{B}_n\,\mathbf{r}$, where $\boldsymbol{B}_n = \mathrm{Diag}\{b_{0,n}, b_{1,n}, \ldots, b_{R,n}\}$, with $b_{0,n}$ being a dummy variable indicating that $\mathcal{S}$ is always on, i.e., $b_{0,n} = 1$, $\forall n$. From this output, the detected symbol $\hat{s}$ is obtained as $\hat{s} = \arg\{\max_{s\in S}\,\Re(s^*\,\hat{\mathbf{h}}^H\,\boldsymbol{B}_n\,\mathbf{r})\}$.

When the M-PSK symbol $s = S_l$ is transmitted, the normalized combiner output $D = \hat{\mathbf{h}}^H\,\boldsymbol{B}_n\,\mathbf{r}|_{S_l}/\sqrt{2\,E_s}$ can be expressed using (4) and (7) as

$$D = (\mathbf{h}+\mathbf{e})^H\,\boldsymbol{B}_n\,(S_l\,\mathbf{V}\,\mathbf{h} + \mathbf{u}) = D_\rho + \jmath\,D_\iota\,, \tag{10}$$

where $D_\rho = \Re(D)$, $D_\iota = \Im(D)$, $\mathbf{u} = \mathbf{n}/\sqrt{2\,E_s}$ is independent of $\mathbf{e}$ and $\mathbf{u} \sim \mathcal{CN}(\mathbf{0}_{L_0\,(R+1)}, \gamma^{-1}\,\mathbf{I}_{L_0\,(R+1)})$, with $\gamma = E_s/N_0$ being the total average signal-to-noise ratio (SNR) per branch and per symbol.

B. Joint CF of Real and Imaginary Parts of MRC Output

Conditioned on $\mathbf{h}$, the two vectors consisting the inner product in (10), i.e., $\mathbf{x} = \mathbf{h}+\mathbf{e}$ and $\mathbf{y} = S_l\,\mathbf{V}\,\mathbf{h} + \mathbf{u}$, are complex Gaussian and mutually independent, with $\mathbf{x} \sim \mathcal{CN}(\mathbf{h}, \gamma_{\rm p}^{-1}\,\mathbf{V}^{-2})$ and $\mathbf{y} \sim \mathcal{CN}(S_l\,\mathbf{V}\,\mathbf{h}, \gamma^{-1}\,\mathbf{I}_{L_0\,(R+1)})$. Thus, by applying the Theorem 1 and by averaging over $\mathbf{h}$, the joint CF of D_ρ and D_ι, is given by (11) (at top of the next page).

C. Asymptotic ASEP Expression of $\mathcal{E}_{\boldsymbol{h}}\left\langle P_{se,\mathcal{D}}|\mathbf{b}_n\right\rangle$

For arbitrary M we assume that S_0 is transmitted. Conditioned on $\mathbf{h}$, the probability of symbol error can be obtained as $P_{se,\mathcal{D}} = \Pr\{\pi/M \geq \angle D > 2\,\pi - \pi/M\}$. Using (10), (11), and [8, eqs. (39) and (43)] for high SNR ($\gamma, \gamma_{\rm p} \gg 1$), an approximate M-PSK ASEP expression yields

$$\mathcal{E}_{\mathbf{h}}\left\langle P_{se,\mathcal{D}}|\mathbf{b}_n\right\rangle \approx \frac{1}{\pi}\int_0^{\frac{\pi(M-1)}{M}}\prod_{\ell=0}^{R}\Psi_{\|\mathbf{h}_\ell\|^2}^{b_{\ell,n}}\left(-\frac{\lambda_\ell\,\gamma\,\gamma_{\rm p}}{\gamma+\gamma_{\rm p}}\,\frac{\sin^2(\pi/M)}{\sin^2(\alpha)}\right)\mathrm{d}\alpha\,. \tag{12}$$

It can be easily verified that for a fixed value of $\gamma_{\rm p}$ and as $\gamma\to\infty$, $\mathcal{E}_{\mathbf{h}}\left\langle P_{se,\mathcal{D}}|\mathbf{b}_n\right\rangle$ tends to an irreducible error floor.

D. Derivation of $\mathcal{E}_{\mathbf{g}_p}\left\langle P_{se,\mathcal{R}_p}\right\rangle$ From $\mathcal{E}_{\boldsymbol{h}}\left\langle P_{se,\mathcal{D}}|\mathbf{b}_n\right\rangle$

As already mentioned in Section III, all the preceding analysis has been performed with respect to (3b). However, the e2e ASEP in (8) also requires $\mathcal{E}_{\mathbf{g}_p}\left\langle P_{se,\mathcal{R}_p}\right\rangle$ with respect to (3a). In order to be able to extract $\mathcal{E}_{\mathbf{g}_p}\left\langle P_{se,\mathcal{R}_p}\right\rangle$ from $\mathcal{E}_{\mathbf{h}}\left\langle P_{se,\mathcal{D}}|\mathbf{b}_n\right\rangle$, the substitutions of all those pairs of symbols provided in Table I should be performed. Using (12), $\mathcal{E}_{\mathbf{g}_p}\left\langle P_{se,\mathcal{R}_p}\right\rangle$ is extracted as

$$\mathcal{E}_{\mathbf{g}_p}\left\langle P_{se,\mathcal{R}_p}\right\rangle \approx \frac{1}{\pi}\int_0^{\frac{\pi(M-1)}{M}}\Psi_{\|\mathbf{g}_p\|^2}\left(-\frac{\lambda_\ell\,\gamma\,\gamma_{\rm p}}{\gamma+\gamma_{\rm p}}\,\frac{\sin^2\left(\frac{\pi}{M}\right)}{\sin^2(\alpha)}\right)\mathrm{d}\alpha\,. \tag{13}$$

$$\Psi_{D_\rho,D_\iota}(\jmath\,\omega_1,\jmath\,\omega_2)=\prod_{\ell=0}^{R}\Psi_{\|\mathbf{h}_\ell\|^2}^{b_{\ell,n}}\left\{-\frac{\left(\omega_1^2+\omega_2^2\right)\,\frac{\gamma+\gamma_{\rm p}}{4\,\gamma\,\gamma_{\rm p}}-\jmath\,\sqrt{\lambda_\ell}\,(\omega_1+\omega_2)}{1+\frac{\omega_1^2+\omega_2^2}{4\,\lambda_\ell\,\gamma\,\gamma_{\rm p}}}\right\}\left(1+\frac{\omega_1^2+\omega_2^2}{4\,\lambda_\ell\,\gamma\,\gamma_{\rm p}}\right)^{-b_{\ell,n}\,L_0} \tag{11}$$

TABLE I
SUBSTITUTION PAIRS FOR DERIVING $\mathcal{E}_{\mathbf{g}_p}\langle P_{se,\mathcal{R}_p}\rangle$ FROM $\mathcal{E}_{\mathbf{h}}\langle P_{se,\mathcal{D}}|\mathbf{b}_n\rangle$

Current Formula Based on (3b)	New Formula Based on (3a)	Where to Apply
$\mathbf{h}_\ell$	$\mathbf{g}_p$	Sections IV-B, IV-C, and V
L_0	L_p	
λ_ℓ	λ_0	
$\sum_{\ell=0}^{R}$ or $\prod_{\ell=0}^{R}$	–	
$b_{\ell,n}$	1	
m_ℓ	κ_p	Section V
$\Omega_{\ell,i}$	$\Theta_{p,i}$	
$\epsilon_{i,\ell}$	$\varepsilon_{i,p}$	
$q_{i,\ell}$	$\upsilon_{i,p}$	
N_ℓ	$\mathcal{N}_p$	
$\nu_{k\ell1}$, $\nu_{k\ell2}$	ν_{kp1}, ν_{kp2}	

E. Optimal Power Allocation

In order to minimize the e2e ASEP, optimum power allocation (OPA) can be succeeded using (8), (12) and (13) as

$$\boldsymbol{\lambda}_{\rm opt}=\arg\min_{\boldsymbol{\lambda}}\left\{P_{se,e2e}\right\}, \tag{14}$$

subject to $\sum_{\ell=0}^{R}\lambda_\ell=1$ and $0<\lambda_\ell<1$, $\forall\ell=0,1,\ldots,R$, with $\boldsymbol{\lambda}=[\lambda_0\,\lambda_1\cdots\lambda_R]^T$ being the power allocation vector.

In general, the above nonlinear optimization problem can be only solved based on numerical techniques. Hence, a generic analytical solution can not be derived.

V. A CASE STUDY: CORRELATED NAKAGAMI FADING

When the receive channels of $\mathcal{D}$, $\mathbf{h}_\ell$, are subject to correlated Nakagami fading, the CF of of $\|\mathbf{h}_\ell\|^2=\sum_{i=1}^{L_0}|h_{\ell,i}|^2$ is

$$\Psi_{\|\mathbf{h}_\ell\|^2}(\jmath\,\omega)=\prod_{i=1}^{N_\ell}\left(1-\jmath\,\omega\,\frac{\epsilon_{i,\ell}}{m_\ell}\right)^{-m_\ell\,q_{i,\ell}}, \tag{15}$$

with $m_\ell\geq 0.5$ being the Nakagami fading parameter and $\mathrm{tr}\left(\mathcal{E}\left\langle\mathbf{h}_\ell\,\mathbf{h}_\ell^H\right\rangle\right)=\mathcal{E}\left\langle\|\mathbf{h}_\ell\|^2\right\rangle=\sum_{i=1}^{L_0}\Omega_{\ell,i}$. In (15), $\epsilon_{i,\ell}$'s denote N_ℓ distinct eigenvalues of matrix $\mathbf{K}_{h_\ell}$ having multiplicities $q_{i,\ell}$ $(i=1,2,\ldots,N_\ell)$, with $\sum_{i=1}^{N_\ell}q_{i,\ell}=L_0$ and $\sum_{i=1}^{N_\ell}q_{i,\ell}\,\epsilon_{i,\ell}=\sum_{i=1}^{L_0}\Omega_{\ell,i}$, while $\epsilon_{i,\ell}>0$ $\forall i,\ell$. From (12) and (15), a high-SNR ASEP expression for M-PSK yields

$$\mathcal{E}_{\mathbf{h}}\langle P_{se,\mathcal{D}}|\mathbf{b}_n\rangle\approx\frac{1}{\pi}\int_0^{\pi\frac{M-1}{M}}\prod_{\ell=0}^{R}\prod_{i=1}^{N_\ell}\left(1+\lambda_\ell\,\frac{\gamma\,\gamma_{\rm p}}{\gamma+\gamma_{\rm p}}\times\frac{\epsilon_{i,\ell}}{m_\ell}\,\frac{\sin^2(\pi/M)}{\sin^2(\alpha)}\right)^{-b_{\ell,n}\,m_\ell\,q_{i,\ell}}\mathrm{d}\alpha\,. \tag{16}$$

Also, using Table I, (16) is transformed as

$$\mathcal{E}_{\mathbf{g}_p}\left\langle P_{se,\mathcal{R}_p}\right\rangle\approx\frac{1}{\pi}\int_0^{\pi\frac{M-1}{M}}\prod_{i=1}^{N_p}\left(1+\lambda_0\,\frac{G\,\varepsilon_{i,p}/\kappa_p}{\sin^2(\alpha)}\right)^{-\kappa_p\,\upsilon_{i,\ell}}\mathrm{d}\alpha\,, \tag{17}$$

with $G=\frac{\gamma\,\gamma_{\rm p}}{\gamma+\gamma_{\rm p}}\,\sin^2(\frac{\pi}{M})$, $\varepsilon_{i,p}$'s and $\upsilon_{i,p}$'s being respectively $\mathcal{N}_p$ positive eigenvalues and their multiplicities of the $\mathcal{S}\to\mathcal{R}_p$ Nakagami channel and κ_p being the fading parameter.

Although (16) and (17), and thus (8), can be easily evaluated using numerical integration techniques, some insights of these expressions can be revealed as follows. Let $x_{i,\ell}=G\,\lambda_\ell\,\frac{\epsilon_{i,\ell}}{m_\ell}$. Based on (16) it can be easily proved that

$$\begin{aligned}I_\zeta&=\lim_{\substack{x_{i,\ell}\to\infty\\ \forall i,\ell}}\left(\prod_{\ell=0}^{R}\prod_{i=1}^{N_\ell}x_{i,\ell}^{b_{\ell,n}\,m_\ell\,q_{i,\ell}}\right)\mathcal{E}_{\mathbf{h}}\langle P_{se,\mathcal{D}}|\mathbf{b}_n\rangle\\&=\frac{1}{\pi}\left[\frac{\sqrt{\pi}}{2}\,\frac{\Gamma\left(\frac{1}{2}+\zeta\right)}{\Gamma\left(1+\zeta\right)}-\xi\,{}_2F_1\left(\frac{1}{2},\frac{1}{2}-\zeta;\frac{3}{2};\xi^2\right)\right],\end{aligned} \tag{18}$$

with $\xi=\cos(\pi\,\frac{M-1}{M})$, $\zeta=L_0\,\sum_{\ell=0}^{R}b_{\ell,n}\,m_\ell$, and with $\Gamma(\cdot)$ and ${}_2F_1(\cdot,\cdot;\cdot;\cdot)$ being the Gamma and Gauss hypergeometric functions, respectively. Using (16) and (18), a closed-form ASEP expression yields

$$\mathcal{E}_{\mathbf{h}}\langle P_{se,\mathcal{D}}|\mathbf{b}_n\rangle=I_\zeta\,G^{-\zeta}\prod_{\ell=0}^{R}\frac{\lambda_\ell^{-b_{\ell,n}\,m_\ell\,L_0}}{\prod_{i=1}^{N_\ell}\left(\epsilon_{i,\ell}/m_\ell\right)^{b_{\ell,n}\,m_\ell\,q_{i,\ell}}}, \tag{19}$$

while using Table I, (19) is transformed as

$$\mathcal{E}_{\mathbf{g}_p}\left\langle P_{se,\mathcal{R}_p}\right\rangle=\frac{I_{\kappa_p\,L_p}\,G^{-\kappa_p\,L_p}}{\prod_{i=1}^{\mathcal{N}_p}\left(\varepsilon_{i,p}/\kappa_p\right)^{\kappa_p\,\upsilon_{i,p}}}\,\frac{1}{\lambda_0^{\kappa_p\,L_p}}\,. \tag{20}$$

The last two expressions are quite useful because they include λ_ℓ's as separate power product terms. Their specific form simplify the analysis for the OPA, while provide information concerning the cooperation-gain and diversity-order.

A. Cooperation-Gain and Diversity-Order

When $\gamma,\gamma_{\rm p}\to\infty$, i.e., $G\to\infty$, e2e approximate ASEP expressions can be obtained for two meaningful limiting cases that are $L_0\geq L_p$ and $L_0\leq L_p$ $\forall p=1,2,\ldots,R$. By substituting (19) and (20) in (8), and using the hint that $\Pr\{\mathcal{R}_p:\ \mathrm{on/off}|b_{p,n}=1\}\simeq 1$ in (9), the e2e ASEP can be accurately approximated as

$$P_{se,e2e}\simeq\sum_{n=0}^{2^R-1}\frac{\mathcal{A}_n}{G^{m\,L_0+m\,\sum_{p=1}^{R}[b_{p,n}\,L_0+(1-b_{p,n})\,L_p]}}, \tag{21}$$

where $m_\ell=\kappa_p=m$ $\forall\ell,p$, $\mathcal{A}_n>0$. The dominant term in this sum as $G\to\infty$ will be the one that is in the lowest power of G. It can be easily verified that for $L_0\geq L_p$ and $L_0\leq L_p$, the corresponding terms are for network states $\mathbf{b}_0$ and $\mathbf{b}_{2^R-1}$. Hence, the e2e M-PSK ASEPs can be approximated as

$$\begin{aligned}P_{se,e2e}\simeq&\frac{I_{L_0\,m}\,\lambda_0^{-m\,\sum_{\ell=0}^{R}L_\ell}}{\prod_{i=1}^{N_0}\left(\epsilon_{i,0}/m\right)^{m\,q_{i,0}}}\\&\times\left[\prod_{p=1}^{R}\frac{I_{L_p\,m}}{\prod_{i=1}^{N_p}\left(\frac{\varepsilon_{i,p}}{m}\right)^{m\,\upsilon_{i,p}}}\right]\,\frac{1}{G^{m\,\sum_{\ell=0}^{R}L_\ell}},\end{aligned} \tag{22a}$$

when $L_0 \geq L_p$ and

$$P_{se,e2e} \simeq \frac{I_{m\,L_0\,(R+1)} \prod_{\ell=0}^{R} \lambda_\ell^{-m\,L_0}}{\prod_{\ell=0}^{R} \prod_{i=1}^{N_\ell} \left(\frac{\epsilon_{i,\ell}}{m}\right)^{m\,q_{i,\ell}}} \frac{1}{G^{m\,L_0\,(R+1)}}\,, \quad (22b)$$

when $L_0 \leq L_p$. The cooperation-gain and diversity-order ($\mathcal{G}_c$ and $\mathcal{G}_d$) can be obtained from the e2e ASEP as $P_{se,e2e} = \lim_{\gamma\to\infty} (\mathcal{G}_c/\gamma)^{\mathcal{G}_d}$. For $\gamma_{\rm p} \to \infty$, i.e., $G \simeq \gamma \sin^{-2}(\pi/M)$, when $L_0 \geq L_p$,

$$\mathcal{G}_c = \frac{\sin^2(\pi/M)}{\lambda_0} \left[\frac{I_{L_0\,m}}{\prod_{i=1}^{N_0} (\epsilon_{i,0}/m)^{m\,q_{i,0}}} \times \prod_{p=1}^{R} \frac{I_{L_p\,m}}{\prod_{i=1}^{N_p} (\varepsilon_{i,p}/m)^{m\,v_{i,p}}} \right]^{1/(m\,\sum_{\ell=0}^{R} L_\ell)} \quad (23a)$$

and $\mathcal{G}_d = m \sum_{\ell=0}^{R} L_\ell$, while when $L_0 \leq L_p$,

$$\mathcal{G}_c = \sin^2\left(\frac{\pi}{M}\right) \times \left[I_{m\,L_0\,(R+1)} \prod_{\ell=0}^{R} \frac{\lambda_\ell^{-m\,L_0}}{\prod_{i=1}^{N_\ell} (\epsilon_{i,\ell}/m)^{m\,q_{i,\ell}}} \right]^{1/(m\,L_0\,(R+1))} \quad (23b)$$

and $\mathcal{G}_d = m\,L_0\,(R+1)$. By comparing the results for the above two cases, we may conclude that the e2e performance for high SNR depends mainly on the characteristics of the "less" channels hop. It should be noted that based on (21) or (22), for a fixed $\gamma_{\rm p}$, i.e., $G \simeq \gamma_{\rm p}\, \sin^{-2}(\pi/M)$, the diversity-order approaches to zero due to the error floor.

B. Optimal Power Allocation for $R = 1$

Here we consider one relay. Using (8), (19), and (20) for independent and identically distributed Nakagami fading with $L_\ell = L$ and $m_\ell = \kappa_p = m$, $\forall \ell, p$, the asymptotic e2e ASEP is given by

$$P_{se,e2e} = \frac{G^{-2\,m\,L}}{\left(\frac{\Omega_{sd}}{m}\right)^{m\,L}} \left[\frac{I_L^2}{\left(\frac{\Omega_{sr}}{m}\right)^{m\,L} \lambda_0^{2\,m\,L}} + \frac{I_{2\,L}}{\left(\frac{\Omega_{rd}}{m}\right)^{m\,L} \lambda_0^{m\,L}\,\lambda_1^{m\,L}} - \frac{G^{-m\,L}\, I_{2\,L}\, I_L}{\left(\frac{\Omega_{sr}}{m}\,\frac{\Omega_{rd}}{m}\right)^{m\,L} \lambda_0^{2\,m\,L}\,\lambda_1^{m\,L}} \right], \quad (24)$$

where $\Omega_{0,i} = \Omega_{sd}$, $\Theta_{1,i} = \Omega_{sr}$ and $\Omega_{1,i} = \Omega_{rd}$ stand for the $\mathcal{S} \to \mathcal{D}$, $\mathcal{S} \to \mathcal{R}_1$, and $\mathcal{R}_1 \to \mathcal{D}$ channel powers, respectively. Using (24), the optimization problem in (14), with respect to λ_0 and $\lambda_1 = 1 - \lambda_0$, can be easily solved using standard minimization techniques. Starting with $\mathrm{d}P_{se,e2e}(\lambda_0)/\mathrm{d}\lambda_0 = 0|_{\lambda_0=\hat{\lambda}_0}$, and after some algebraic manipulations, we have

$$\hat{\lambda}_0^{m\,L} \frac{(2\,\hat{\lambda}_0 - 1)\, I_{2\,L}}{(\Omega_{rd}/m)^{m\,L}} + (3\,\hat{\lambda}_0 - 2) \frac{G^{-m\,L}\, I_{2\,L}\, I_L}{(\Omega_{sr}\,\Omega_{rd}/m^2)^{m\,L}} = \frac{2\, I_L^2}{(\Omega_{sr}/m)^{m\,L}} (1 - \hat{\lambda}_0)^{m\,L+1}\,. \quad (25)$$

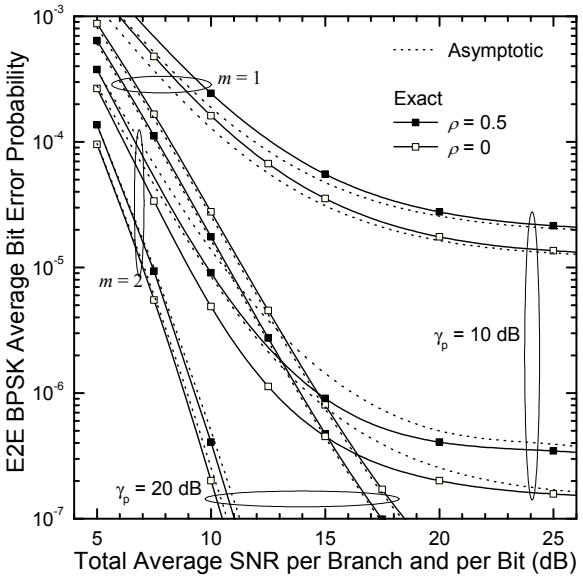

Fig. 1. E2e ABEP of BPSK versus average SNR, γ, for $R = 1$ and different $\gamma_{\rm p}$, m, ρ.

Well-known root-finding techniques for polynomials must be applied in order to get a real root for $\hat{\lambda}_0$ in $(0, 1)$. Note that Ω_{sd} does not have any impact on the optimization of the power.

VI. Numerical Results and Conclusions

We shall consider identical channel models for all hops, same number of receive antennas, $L_\ell = L\ \forall \ell = 0, 1, \ldots, R$, and $\Omega_{sd} = \Omega_{sr} = \Omega_{0,j} = \Theta_{p,j} = 1$ and $\Omega_{rd} = \Omega_{p,j} = 10$ $\forall p = 1, 2, \ldots, R$ and $j = 1, 2, \ldots, L$. Moreover, for correlated fading channels, the exponential correlation model is adopted $\varrho_{p,i,j} = \rho_{\ell,i,j} = \rho^{|i-j|}\ \forall i, j = 1, 2, \ldots, L$, while identical Nakagami fading parameters, $m_\ell = m\ \forall \ell$, are assumed.

In Fig. 1 asymptotic results (dotted curves) for the exact e2e ABEP of a BPSK pilot-symbols assisted system versus the total average SNR per branch and per bit are presented using (8) with (16)–(17), for a dual-hop system with a single relay ($R = 1$), $\lambda_0 = 0.7$ and $\lambda_1 = 0.3$, dual-branch MRC ($L = 2$), correlated Nakagami fading and different values for the average PNR per pilot sequence and per time slot, $\gamma_{\rm p}$, Nakagami fading parameter, m, and correlation coefficient, ρ. It is obvious that the ABEP performance significantly improves as γ, $\gamma_{\rm p}$ and/or m increase. Clearly, an increase of $\gamma_{\rm p}$ reduces the error floor. Based on [16], exact results (solid curves) are also included in the same figure in order to verify the accuracy of our high-SNR approximations. From the comparison it can be easily verified that (16) and (17) are highly accurate.

Similar conclusions can be drawn from Fig. 2, where e2e QPSK ASEP curves are presented as a function of the total average SNR per branch and per symbol for $\gamma_{\rm p} = 10$ dB, $R = 2$, $\lambda_0 = 0.5$, $\lambda_1 = 0.3$ and $\lambda_2 = 0.2$, and different values of L, ρ, and m. Both asymptotic and exact curves are included for comparison purposes using (8) with (16)–(17) and [16], respectively. As shown, the higher the m and L are, the better

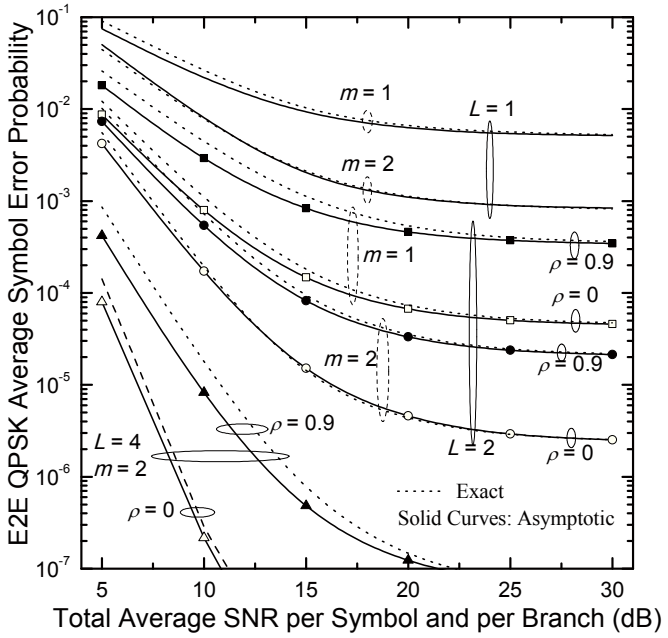

Fig. 2. E2e ASEP of QPSK versus total average SNR, γ, for $\gamma_{\rm p} = 10$ dB, $R = 2$, exponentially correlated Nakagami fading and different L, ρ, m.

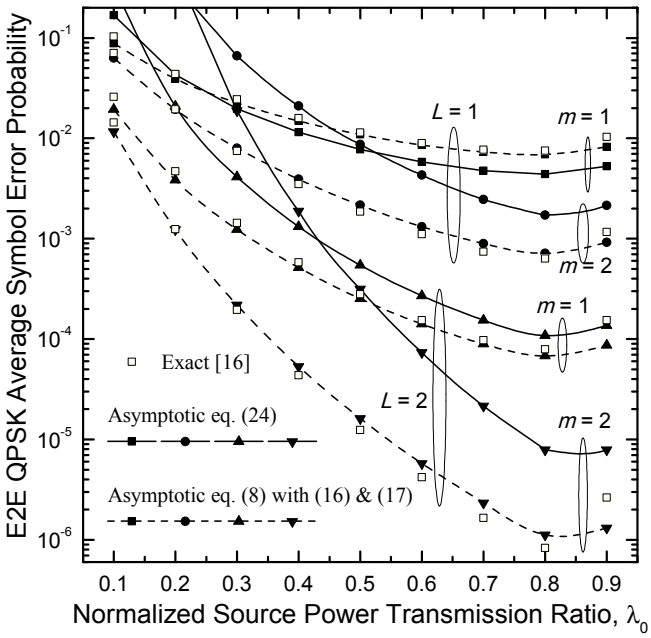

Fig. 3. E2e ASEP of QPSK versus normalized source transmit power ratio, λ_0, for $\gamma = \gamma_{\rm p} = 15$ dB, $R = 1$, $\gamma = 15$ dB, and different L, m.

performance is achieved. Moreover, the ASEP performance is significantly degraded when the channels are highly correlated. Once again note the accuracy of the asymptotic curves.

In Fig. 3 asymptotic e2e ASEP curves of QPSK versus λ_0 are presented (using (8) with (16)–(17) and (24)) for a dual-hop system, $\gamma = \gamma_{\rm p} = 15$ dB, $R = 1$, independent Rayleigh fading, and different values of L and m. From this figure we observe that (24), and thus, (25) is highly accurate in finding the optimum λ_0 that minimizes the e2e ASEP. This conclusion is further supported from the comparison with exact results (square signs) [16].

ACKNOWLEDGMENT

Dr. Sagias work was supported by the University of Peloponnese in the context of the internal project ODesRI.

REFERENCES

[1] K. J. R. Liu, A. K. Sadek, W. Su, and A. Kwasinski, *Cooperative Communications and Networking*. UK: Cambridge University Press, Jan. 2009.

[2] J. Proakis and M. Salehi, *Digital Communications*, 5th ed. New York, USA: McGraw-Hill, 2007.

[3] R. F. Pawula, S. O. Rice, and J. H. Roberts, "Distribution of the phase angle between two vectors perturbed by Gaussian noise," *IEEE Trans. Commun.*, vol. COM-30, no. 8, pp. 1828–1841, Aug. 1982.

[4] R. F. Pawula, "Distribution of the phase angle between two vectors perturbed by Gaussian noise II," *IEEE Trans. Veh. Technol.*, vol. 50, no. 2, pp. 576–583, Mar. 2001.

[5] W. M. Gifford, M. Z. Win, and M. Chiani, "Diversity with practical channel estimation," *IEEE Trans. Wireless Commun.*, vol. 4, no. 5, pp. 1935–1947, Jul. 2005.

[6] Y. Ma, R. Schober, and S. Pasupathy, "Effect of channel estimation errors on MRC diversity in Rician fading channels," *IEEE Trans. Veh. Technol.*, vol. 54, no. 6, pp. 2137–2142, Nov. 2005.

[7] J. M. Torrance and L. Hanzo, "Comparative study of pilot symbol assisted modem schemes," in *Proc. IEE Radio Receiv. Assoc. System Conf. (RRAS)*, Bath, UK, Sep. 1995.

[8] R. K. Mallik and N. C. Sagias, "Distribution of inner product of complex Gaussian random vectors and its applications," *IEEE Trans. Commun.*, vol. 59, no. 12, pp. 3353–3362, Dec. 2011.

[9] S. Han, S. Ahn, E. Oh, and D. Hong, "Effect of channel-estimation error on BER performance in cooperative transmission," *IEEE Trans. Veh. Technol.*, vol. 58, no. 4, p. 20832088, May 2009.

[10] M. J. Taghiyar, S. Muhaidat, and J. Liang, "On the performance of pilot symbol assisted modulation for cooperative systems with imperfect channel estimation," in *Proc. IEEE Wirel. Commun. Networking Conf. (WCNC'10)*, Sydney, Australia, Apr. 2010.

[11] X. J. Zhang and Y. Gong, "On the diversity gain in dynamic decode-and-forward channels with imperfect CSIT," *IEEE Trans. Commun.*, vol. 59, no. 1, pp. 59–63, Jan. 2011.

[12] D. S. Michalopoulos, N. D. Chatzidiamantis, R. Schober, and G. K. Karagiannidis, "Relay selection with outdated channel estimates in Nakagami-m fading," in *Proc. IEEE Internat. Conf. Commun. (ICC'11)*, Kyoto, Japan, Jun. 2011.

[13] O. Amin, S. S. Ikki, and M. Uysal, "On the performance analysis of multirelay cooperative diversity systems with channel estimation errors," *IEEE Trans. Veh. Technol.*, vol. 60, no. 5, pp. 2050–2059, Jun. 2011.

[14] S. S. Ikki, S. Al-Dharrab, and M. Uysal, "Error probability of DF relaying with pilot-assisted channel estimation over time-varying fading channels," *IEEE Trans. Veh. Technol.*, vol. 61, no. 1, pp. 393–397, Jan. 2012.

[15] R. K. Mallik, "Distribution of inner product of two complex Gaussian vectors and its application to MPSK performance," in *Proc. IEEE Internat. Conf. Commun. (ICC'08)*, Beijing, China, May 2008, pp. 4616–4620.

[16] N. C. Sagias, "On the ASEP of decode-and-forward dual-hop networks with pilot-symbol assisted M-PSK," *IEEE Trans. Commun.*, 2014, accepted for publication.